Sebastian Krohn, Jens Frahm, Alannah Mahler, Henning Dathe, Sam Sedaghat, Dietmar Kubein-Meesenburg, Florian Linss, Torsten Wassmann, Ralf Bürgers

Biomechanical analysis of temporomandibular joint dynamics based on real-time magnetic resonance imaging

Abstract

Aim: The traditional hinge axis theory of temporomandibular joint (TMJ) dynamics is increasingly being replaced by the theory of instantaneous centers of rotation (ICR). Typically, ICR determinations are based on theoretical calculations or three-dimensional approximations of finite element models.
Materials and methods: With the advent of real-time magnetic resonance imaging (MRI), natural physiologic movements of the TMJ may be visualized with 15 frames per second. The present study employs real-time MRI to analyze the TMJ biomechanics of healthy volunteers during mandibular movements, with a special emphasis on horizontal condylar inclination (HCI) and ICR pathways. The Wilcoxon rank sum test was used to comparatively analyze ICR pathways of mandibular opening and closure.
Results: Mean HCI was 34.8 degrees (± 11.3 degrees) and mean mandibular rotation was 26.6 degrees (± 7.2 degrees). Within a mandibular motion of 10 to 30 degrees, the resulting x- and y-translation during opening and closure of the mandible differed significantly (10 to 20 degrees, x: $P = 0.02$ and y: $P < 0.01$; 20 to 30 degrees, x: $P < 0.001$ and y: $P = 0.01$). Rotation of both 0 to 10 degrees and > 30 degrees showed no significant differences in x- and y-translation. Near occlusion movements differed only for y-translation ($P < 0.01$).
Conclusion: Real-time MRI facilitates the direct recording of TMJ structures during physiologic mandibular movements. The present findings support the theory of ICR. Statistics confirmed that opening and closure of the mandible follow different ICR pathways, which might be due to muscular activity discrepancies during different movement directions. ICR pathways were similar within maximum interincisal distance (MID) and near occlusion (NO), which might be explained by limited extensibility of tissue fibers (MID) and tooth contact (NO), respectively.

Keywords: *temporomandibular joint, jaw dynamics, biomechanics, real-time magnetic resonance imaging, instantaneous center of rotation*

Introduction

The initial phase of mouth opening has for a long time been described as a pure rotation of the condyle, whereby the mandible rotates around a constant center of rotation located in or around the intercondylar axis[1-3], depending on measurement technologies and the scientific ideas of biomechanics (Fig 1). More recent studies suggest that the center of rotation is not fixed, but moves during the entire process of mouth opening. Accordingly, the former 'hinge axis theory' was amended by the 'instantaneous center of rotation' (ICR) theory[1,4-6]. While the disc and condyle move anteriorly as a unit, the mandible combines a hinge action (ie, rotation) and a slide action (ie, x- and y-translation)[7]. Although it has been proposed to force the mandible into the most posterior position to generate a pure rotation around a 'terminal hinge axis' during initial mouth opening[8-10], Ferrario et al demonstrated that even this constrained mandibular position gives rise to ICRs instead of one specific hinge axis[4]. So far, the analysis of mandibular movements and the determination of specific rotation axes have been limited to methods ranging from kinesiography/axiography to radiodiagnostics, studies of human autopsy material, static and pseudo-dynamic magnetic resonance imaging (MRI), and finite element analysis (FEA) or other computer-based calculations[4,6,11-17]. However, these techniques hamper the visualization and direct measurement of anatomical structures, especially the temporomandibular joint (TMJ) disc, during dynamic natural movements. For example, kinesiography requires headsets, bite forks or facebows attached to the patient's jaws, although Lotzmann et al showed that even mandibular facebows weighing only 100 g have a marked impact on axiographic pathways[18]. Conventional MRI requires mouth wedges to fix mandibular positions and thus causes significant incongruence between the unnatural passive stretching of the mouth and the true TMJ kinetics. Finite element-based analyses of the human masticatory system have served as powerful tools to characterize the role of the disc and other TMJ tissue, but this technique is limited to indirect calculations based on the approximated natural mechanics of a few individuals[19]. For biomechanical studies of clinical relevance, it

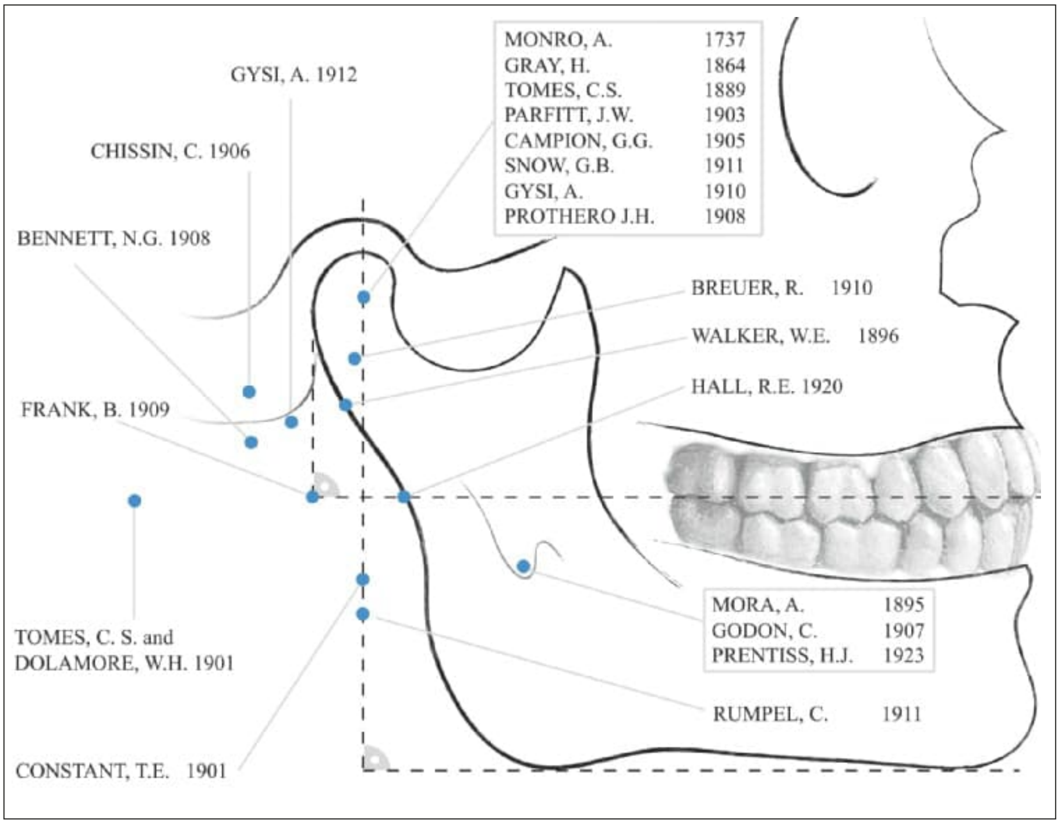

Fig 1 Data from the literature regarding the locations of transverse hinge axes of the mandible during opening movement as proposed by Bosman[37]. Discrepancies of the numerous determinations are due to different measurement technologies and are dependent on the scientific idea of biomechanics.

Video Real-time MRI sequence of the TMJ recorded during habitual movement of the mandible: First, the volunteer's mouth opening begins from the intercuspal position, where the mandibular condyle rests in the glenoid fossa, and then starts to rotate and glide along the articular tubercle. At maximum opening of the jaw, the condyle is located in front of the crest of the articular eminence. The condyle then rotates and glides in the opposite direction toward the glenoid fossa, where it rests at the intercuspal position.

https://video.qvnet.de/ijcd_2020_03_video/ijcd202003vid1.mp4

is essential that mandibular movements are studied under physiologic conditions and are not affected by external devices or mathematical approximation. Recent developments in real-time MRI allow for a unique visualization of all TMJ structures (ie, soft and hard tissue) as well as the assessment of their dynamics (ie, changes in volume and localization) during natural mandibular movements[20-23]. In previous work, the technique has been optimized to yield 15 frames per second at a 0.75×0.75 mm^2 in-plane resolution and 5-mm section thickness. The present study aims to overcome the aforementioned limitations in methodology by using real-time MRI of the TMJ, and to thereby enable reliable biomechanical analyses. In particular, this novel approach offers to derive ICR pathways during natural mouth opening and closure.

Materials and methods

Human rights statement and informed consent

All the procedures followed in this study were in accordance with the ethical standards of the responsible committee on human experimentation (institutional and national) and with the Helsinki Declaration of 1975, as revised in 2008. Informed consent was obtained from all patients included in the study.

Study subjects

The study was approved by the Ethics Committee (project no. 9/4/19An) and all participants provided written informed consent before the MRI. A total of 43 volunteers (23 males, 20 females; 28.7 ± 5.8 years of age, range 23 to 51 years) with sound dentitions, symptomless TMJ function, and without temporomandibular dysfunction (TMD) according to the RDC/TMD criteria, were recruited from the local faculty.

Magnetic resonance imaging

MRI was recorded on a 3.0 Tesla MRI system (Prisma Fit; Siemens Healthcare, Erlangen, Germany) using the standard 64-channel head coil. Real-time MRI with T2/T1 contrast (refocused FLASH) at 15 frames per second was based on a true acquisition time of 66.7 ms per frame. The field of view was 192 × 192 mm, with an in-plane resolution of 0.75 × 0.75 mm, and a section thickness of 5 mm. The gradient-echo time TE was 2.15 ms, and the flip angle was 35 degrees (see supplementary video).

All measurements (n = 86 for both TMJs of 43 subjects) were performed in the supine position. During the MRI, a timing protocol with a schematic visualization of mouth opening and closure (10 s each) was shown to all subjects – liquid-crystal display (LCD) monitor viewed by mirror atop the head coil – in order to standardize the speed of jaw movement, with a total duration of 60 s (900 images). Previous study results show that a slice thickness of 5 mm is appropriate for real-time MRI measurements of the TMJ. However, the average width of the caput mandibulae is 15 to 20 mm in the mediolateral direction. Thus, real-time MRI sequences were conducted in three adjacent sections during three sequential cycles of mouth opening and closure. This procedure guaranteed that the whole TMJ was recorded for selection of the most appropriate section from an anatomical point of view. For the analysis of biomechanics, the central slice of each TMJ was chosen in all subjects, since this MRI section allowed for the depiction of all essential TMJ structures. All subjects were instructed to carry out maximum mouth opening (MMO) – “open mouth as wide as possible” – starting and ending at the (force-free) intercuspal position (ICP).

Data evaluation

Real-time images with online reconstruction appeared as regular images in the database of the MRI system. For further analyses, MRI film sequences were generated with a 64-bit version of the ImageJ (US National Institutes of Health, Bethesda, Maryland, USA) processing software. After Effects CS5 (Adobe, San José, California, USA) software was applied to achieve image stabilization in each subject for reproducible measurements of the mandible and to avoid displacement artifacts due to movements of the subject’s head. Sagittal motion paths of the center of each condyle (condylar path) were determined for all 300 images of one parasagittal section. Horizontal condylar inclination (HCI) was obtained for all TMJs. In order to assess the rotational and translational movements of the mandible, a second tracking point was located at the oblique ridge of the mandibular ramus directly posterior to the second molar, and rigidly linked to the center of the condyle.

All x- and y-coordinates (in the sagittal and vertical direction) of the two tracking points were exported as comma-separated values (CSVs), and the theory of planar kinematics was applied for the calculation of ICRs. This reduces the x- and y-coordinates to three degrees of freedom, ie, rotation defined as

$$\tan \alpha = \frac{y_2 - y_1}{x_2 - x_1}$$

and the x- and y-coordinates of the origin (here, the center of the condyle). Although the formula for the ICR is usually formulated in complex numbers, it can suitably be rewritten to three real components. Let o_x, o_y, and α be real parameters; then the corresponding velocities

$$v_x = \frac{do_x}{dt}, \; v_y = \frac{do_y}{dt}, \text{ and } \omega = \frac{d\alpha}{dt}$$

have to be calculated first. The formulae for the x- and y-components of the ICR are given by $p_x = o_x - v_y/\omega$ and $p_y = o_y + v_x/\omega$. In theoretical kinematics, a pure translation corresponds to an ICR located in infinity. Thus, in the present approach, calculations were restricted to ICRs in the range of the skull’s dimensions, since these are mathematically valid and clinically relevant. The numerical differentiation and smoothing of the signals were performed using appropriate Savitzky-Golay filters[24].

The use of these filters for numerical differentiation overcomes some typical problems of finite differences[25]. Although finite difference formulas have been thoroughly studied[26], they suffer from the problem of calculating differences of numbers with comparable amounts, which is known to lead to a loss of precision. The original formulas of planar kinematics require the calculation of differential quotients of the type $dx/d\alpha$[27]. The definition is given by the limit

$$\frac{dx}{d\alpha} = \lim_{\Delta\alpha \to 0} \frac{\Delta x}{\Delta \alpha},$$

which is a quotient of the undetermined form

$$\frac{"0"}{"0"}.$$

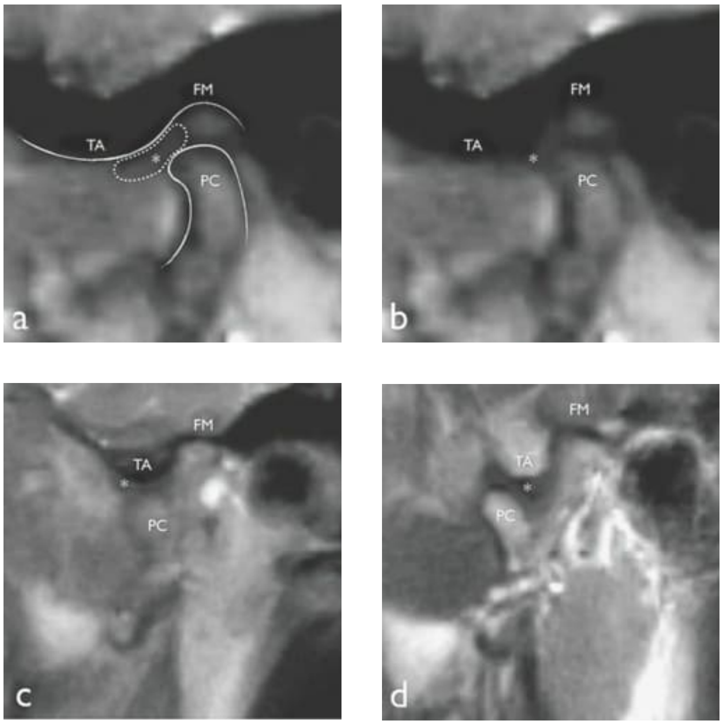

Fig 2 Selected frames from real-time MRI films during mouth opening at intercuspal position (ICP) with markings of the joint surfaces (a), at ICP without markings (b), at about half-open mouth (c), and at maximum open mouth (d). TA = tuberculum articulare; FM = fossa mandibularis; PC = condyle; * = articular disc.

This situation is comparable to the use of the geometrical Reuleaux method of calculating the ICR as a limit of the finite center of rotation (FCR), so that the ICR is located at the intersection of the normals of the point paths. In the present case, L'Hôpital's rule [28] states that such expressions can be evaluated as a quotient of derivatives, here

$$\frac{dx}{d\alpha} = \frac{\dot{x}}{\dot{\alpha}}.$$

This is appropriate for a motion parametrized by time as the only parameter. Now, the differences are replaced by numerical differentiations. This method may be viewed as the attempt to extrapolate to a step size of zero. Savitzky-Golay filters approximate a sample in the neighborhood of the point of interest by a polynomial by least square methods. Afterwards, the polynomial is differentiated analytically, and its derivative evaluated at the point of interest. Thus, no discrete time intervals are needed for the calculation. Furthermore, no subsampling has been applied. Both the number of points in the neighborhood of the point of interest and the degree of the polynomial are free parameters of the Savitzky-Golay filters. In the present dataset, these free parameters have been adjusted such that the path of the ICR is smooth enough to be considered a continuous curve, but not too grossly simplified as a hinge axis. This was undertaken with an eye on several examples before evaluating the entire dataset. The choice of optimal parameters surely depends on the amount and type of data noise.

Statistical analysis

In order to comparatively analyze the direction of mandibular movement, ICR pathways were separately determined for opening and closure movements. By introducing a new categorical variable, respective coordinates were further grouped from 0 to 40 degrees of motion into intervals of 10 degrees of the total rotation angle. No averages were calculated in these groups except for the internal routines of analysis of variances (ANOVAs) or, more generally, linear models. Statistical evaluation was obtained using the Wilcoxon rank sum test, with the continuity correction and significance level set to 5% in statistics software R (version 3.4.3; www.r-project.org). The multiple test adjustment used Holm's method. Descriptive statistics were obtained using XLSTAT (Addinsoft, Paris, France).

Results

Real-time MRI was successfully performed in all 43 subjects and resulted in a mean mandibular mobility of 52.1 mm (± 7.5 mm) and a mean HCI of 34.8 degrees (± 11.3 degrees). The mean mandibular rotation was 26.6 degrees (± 7.2 degrees), while the mean x- and y-translations were 22.9 mm (± 5.8 mm) and 7.9 mm (± 2.8 mm), respectively. All anatomical components of the TMJ could be clearly visualized and distinguished from each other in real-time MRI films at 15 frames per second (n = 86).

As shown in Figure 2, the analyses of moving structures considerably helped to identify and locate the mandibular fossa, articular tubercle, articular disc, and condyle. In the (force-free) ICP, the caput mandibulae of the condyle was typically located in the mandibular fossa and on the posterior half of the articular disc (pars posterior), whereas the disc was located at the transition from the mandibular fossa to the tubercle (Fig 2a and b). The spatial allocation of the condyle and disc changed during mouth opening. When the disc-condyle complex moved over the posterior slope of the tubercle (in the anterior and caudal direction) to reach the eminentia

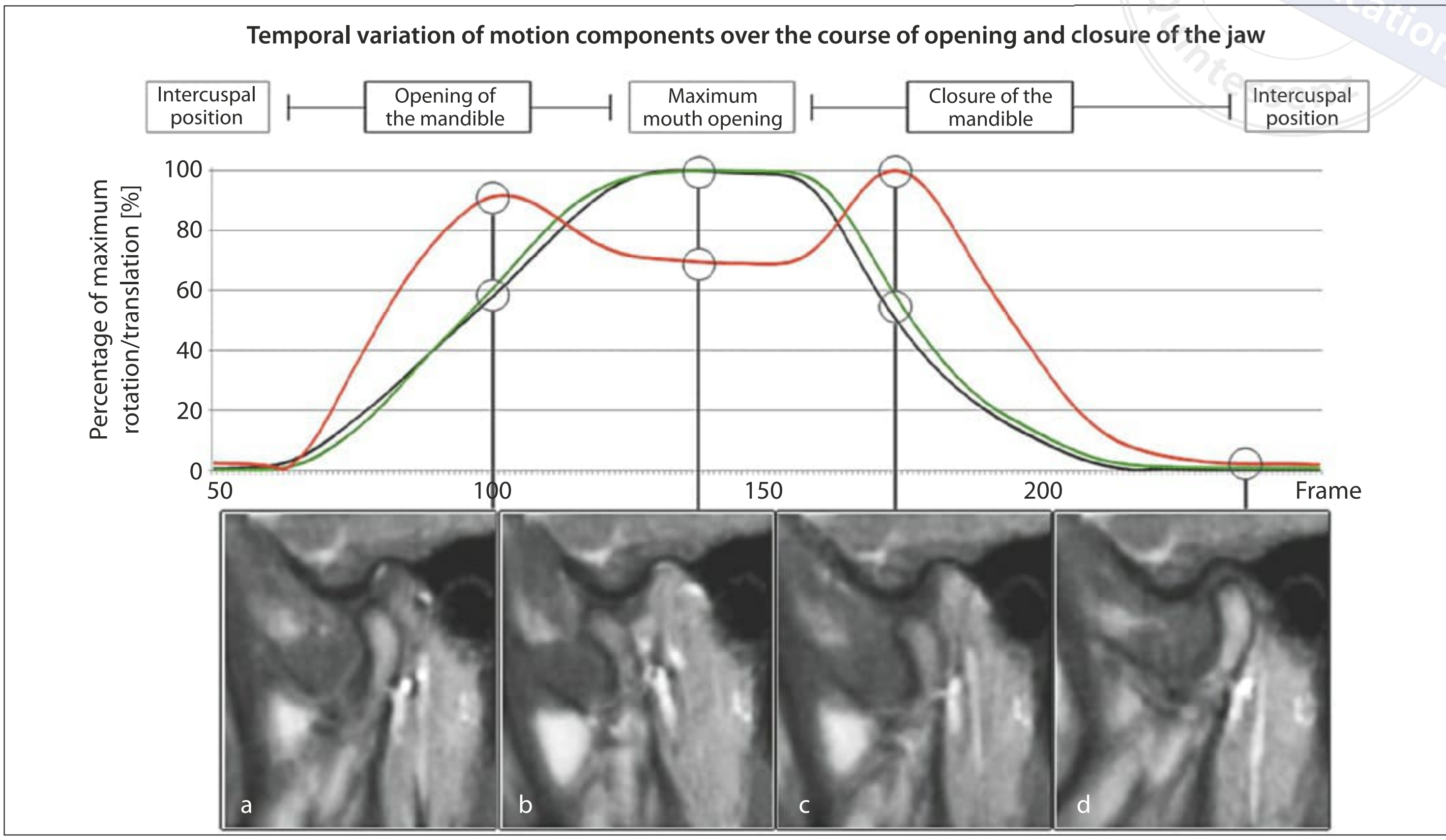

Fig 3 Since the mandible represents a rigid body, the two tracked points (center of the condyle and point on the ramus mandibulae) were permanently linked. Transformation and rotation of this constructed line was measured in a virtual coordinate system with the Frankfort horizontal plane as reference. These calculations led to the following representative translatory and rotatory components of the mandible, as shown in the line graph: The horizontal (abscissa) axis shows the temporal evolution in frames (67 ms resolution, frames 50 to 250), the vertical (ordinate) axis depicts each component as a percentage of its maximum: rotation = black; x-translation = green; y-translation = red. Bottom: Selected real-time images of the TMJ at intermediate mouth opening (a), open mouth (b), intermediate mandibular closure (c), and closed mouth (d).

articularis, the caput mandibulae was mostly located on the intermediary part of the disc (pars intermedia; Fig 2c). Then, the condyle was further pushed to the anterior part of the articular disc (pars anterior) until MMO (Fig 2d). At this endpoint, the condyles moved more or less strongly over the eminence and the anterior slope of the tubercle, back in a cranial direction. As the mandible followed the contour of the tubercle and shifted ventrally (via translation) during mouth opening, the disc also moved forward, even further than the caput mandibulae, due to the force exerted by the simultaneous rotation of the condyle.

The real-time MRI sections selected in the present study enable a comprehensive view of articular disc dynamics during mouth opening and closure in almost all recordings. No partial or total disc dislocation could be observed. In all subjects, the articular discs were located between condyles and tubercles during all phases, indicating 'normal positions' of the disc, according to Orsini, in all cases[29]. While the biconcave character of the disc could be seen during the entire process, the external shape of the disc successively changed (in the sagittal view). The thinnest part of the articular disc shifted from the pars posterior (at the ICP) over the pars intermedia (when the condyle was located on the vertex of the eminentia) to the pars anterior at the MMO. The exact beginning of mouth opening could be determined in every recording. Simultaneous translation and rotation of the condylar process and ramus of the mandible were both observed right from the start of mouth opening in all subjects.

Figure 3 shows the temporal evolution of rotations and of the x- and y-translations during mouth opening and closure of the mandible. Rotation and translation started simultaneously with mouth opening, ie, no initial phase of pure rotation was observed in any patient. Rotations and x-translations

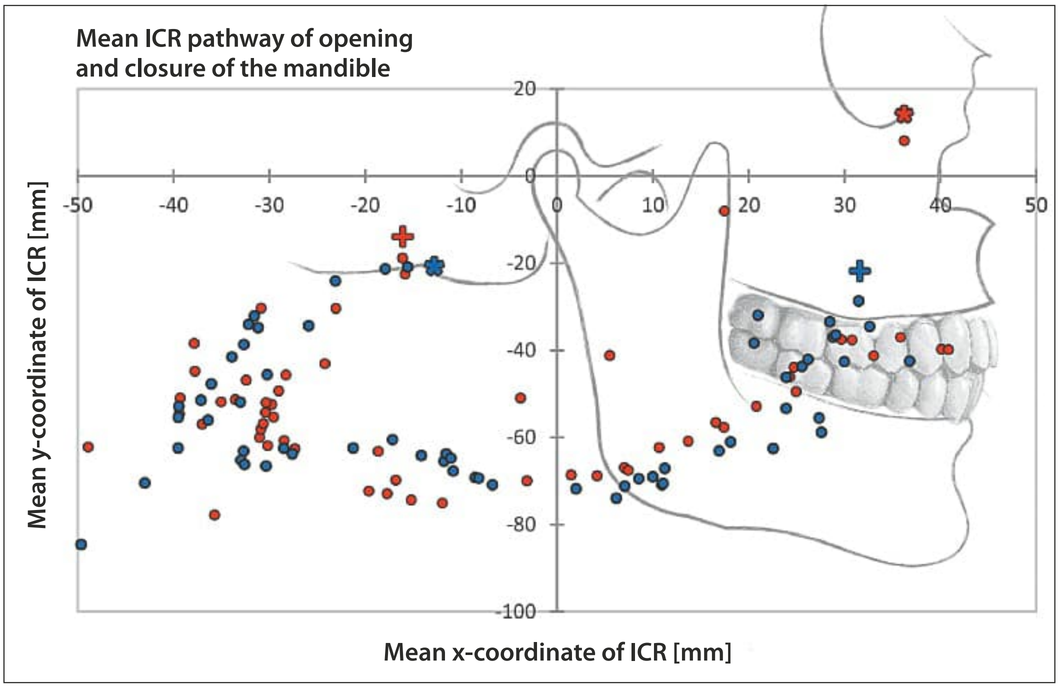

Fig 4 Mean ICR coordinates of all subjects during one full cycle of mouth opening (blue) and closure (red). The first and last ICR of each movement is denoted with a star and cross, respectively. Zero of the coordinate system refers to the condylar center as the origin of all calculations (see the text for details).

occurred congruently during movement, whereas y-translations revealed an incongruous temporal course. During intermediate mouth opening, y-translations reached a sub-maximum peak within the movement of the condyle, slightly before the eminence of the glenoid fossa (Fig 3a). The terminal phase of mouth opening led to the largest values for rotation and x-translation (Fig 3b). At the same time point, the y-translation reached approximately two thirds of its maximum. Maximum y-translation was observed during intermediate jaw closure, whereas values of rotation and x-translation continually decreased (Fig 3c).

Figure 4 shows a high degree of variability for the ICR x- and y-coordinates averaged across the subjects. However, mean ICR pathways of both mandibular opening and closure were never located within the condyle. During initial jaw opening, the ICR pathways started in close spatial proximity, posterior (about 20 mm) to the condyle in all subjects. With increasing mouth opening, the ICRs shifted caudally and posteriorly. Throughout the intermediary phases, the ICR pathways moved horizontally in the anterior direction, but in the terminal phases shifted in the anterior and cranial directions. In general, motion paths were harmonic and predominantly continuous. Apart from a few outliers, the ICRs of mandibular closure lay on a similar path to that of mouth opening, but moved in the opposite direction, ending near the condyle (Fig 4).

The descriptive statistics in Figure 5 reveal the highest values for rotation and x-translation during MMO and initial closure of the mandible, respectively. Mean rotation and x-translation were considerably lower during all other time points. However, y-translation differed remarkably from the other components, since y-translations reached their maximum during both intermediate phases of jaw motion.

In the subgroup of observations between 40 and 50 degrees of mandibular total rotation, which was denoted by the string (-50,-40], only 21 observations occurred. Thus, this group was excluded from the pairwise Wilcoxon tests due to the small sample size. Except for one group comparison, the statistical analysis of all subgroups, which was separately carried out for x- and y-coordinates (Tables 1 and 2, respectively), showed significant differences. Thus, we can clearly speak of a moving ICR. As expected, the comparison of y-coordinates during MMO and ICP showed no significant difference, since the approximation of the condylar path can be described as parabolic, and thus values of the y-coordinates are similar.

The evaluations further demonstrate that ICR coordinates during mandibular opening and closure differ significantly within mandibular motion between 10 to 20 degrees ($P = 0.02$; $P < 0.01$) and 20 to 30 degrees ($P < 0.001$; $P = 0.01$). Between 30 to 40 degrees, no significant differences for x- and y-coordinates were obtained between opening and closure of the mandible ($P = 0.97$; $P = 0.73$). Near occlusion jaw movements in the 0- to 10-degree range show significant differences in y-coordinates ($P < 0.01$), but not in x-coordinates ($P = 0.08$).

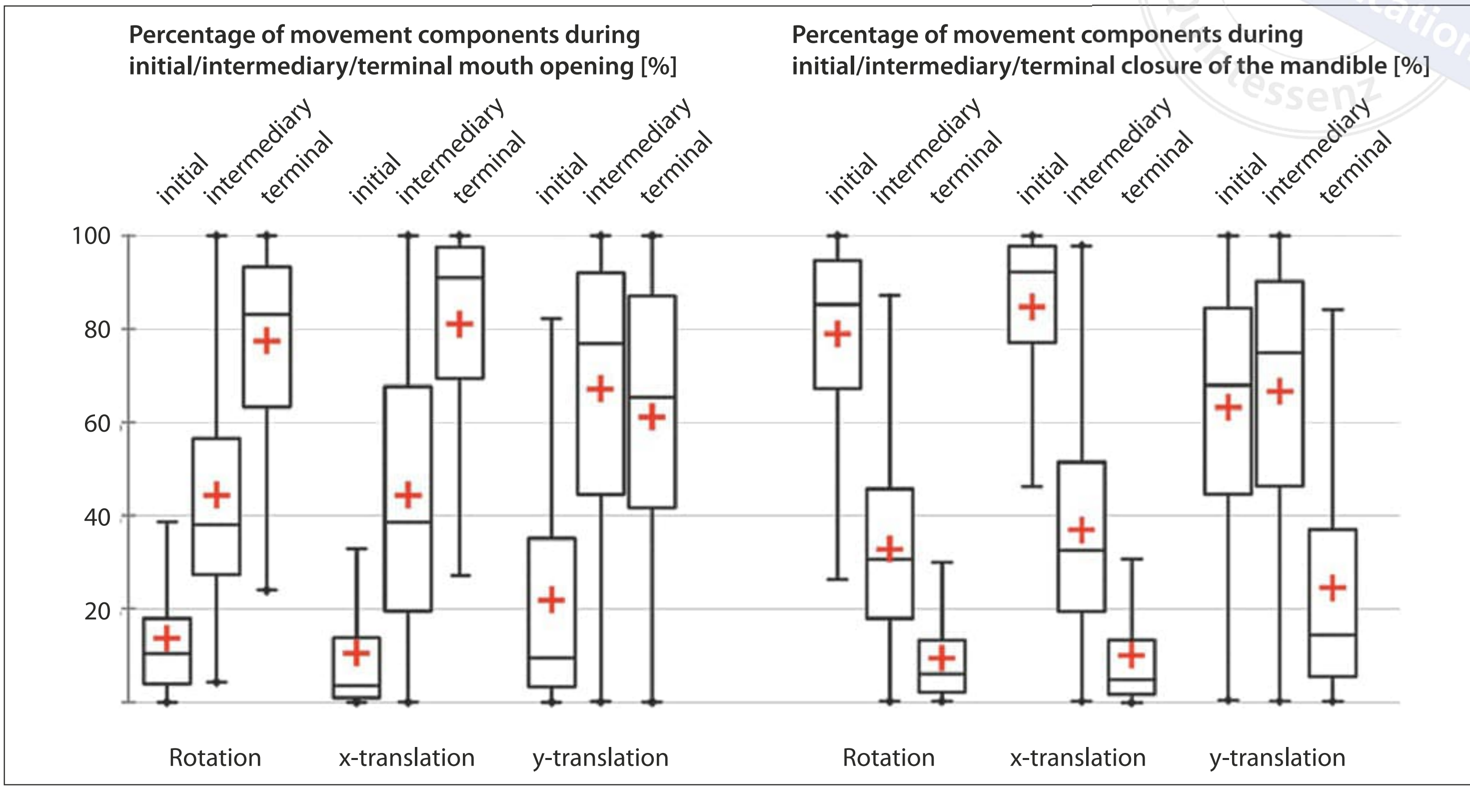

Fig 5 Rotations and translations of all subjects during opening (left) and closure (right) of the mandible at three time points: initial = first 20 real-time MRI images; intermediate = 20 images; and terminal = 20 images. Boxplots depict the percentage of each component's maximum during mandibular movement.

ICRs of near occlusion are particularly relevant for clinical practice, since they represent stereotypical movements from and toward intercuspal contacts, which might be equivalent to chewing patterns. Therefore, ICRs between 0 to 10 degrees of mandibular motion are summarized in Figure 6. The scatterplot shows that ICRs obtained for mouth opening enclose a remarkably larger area compared with those for mandibular closure. Especially in the y-translation, there is a lower ICR variability during mandibular closure, which indicates greater consistency within subjects.

Discussion

Research on TMJ dynamics during natural mandibular movement has hitherto been extremely laborious and mainly based on indirect methods. Using real-time MRI, individual mandibular movements can be observed as subjects simply open and close their mouths under temporal control without any other manipulation, as required by other techniques. Thus, the availability of real-time MRI in the sagittal oblique direction for the first time allows for dynamic visualization

Table 1 Statistical results of x-coordinates of ICR determined by using pairwise Wilcoxon tests for each total rotation subgroup

	(-40,-30]	(-30,-20]	(-20,-10]	(-10,0]
(-30,-20]	2.8e-11	-	-	-
(-20,-10]	< 2e-16	< 2e-16	-	-
(-10,0]	< 2e-16	< 2e-16	< 2e-16	-
(0,10]	< 2e-16	< 2e-16	8.4e-06	< 2e-16

Table 2 Statistical results of y-coordinates of ICR determined by using pairwise Wilcoxon tests for each total rotation subgroup

	(-40,-30]	(-30,-20]	(-20,-10]	(-10,0]
(-30,-20]	< 2e-16	-	-	-
(-20,-10]	< 2e-16	< 2e-16	-	-
(-10,0]	< 2e-16	< 2e-16	< 2e-16	-
(0,10]	0.17	1.2e-07	< 2e-16	< 2e-16

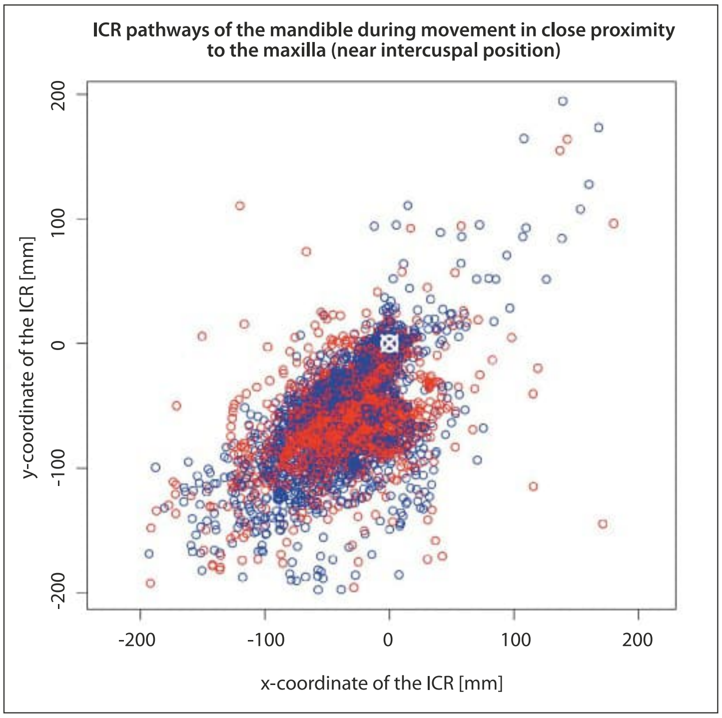

Fig 6 ICR coordinates of all subjects during the first 10 degrees of mouth opening (blue) and the last 10 degrees of mouth closure (red) with the origin (cross).

and the direct measurement of TMJ structures during natural movements[20,21,30]. On the whole, the present real-time MRI findings on ICR pathways are consistent with the axiographic observations of Sadat-Khonsari et al[15,31]. Accordingly, physiologic ICR paths during mouth opening start near the condyle and then move downward backward, and finally shift forward and forward upward. Trajectories of specific points of the mandible during jaw movement were already used in instrumental functional analysis and axiography to describe TMJ biomechanics. For example, such observations were displayed in Posselt's diagram, and then used as hinge axis construction templates for generations of articulators, despite the fact that the reproducibility of determining hinge axes is low[32-34]. In contrast, recent studies indicate that a steady hinge axis during mouth opening does not exist. Instead, mandibular movements during mouth opening and closure combine translation and hinge components, and thus it cannot be compared with a standard hinge joint[4,35]. Here, all real-time MRI films were analyzed via two-point tracking: The corresponding ICR paths clearly indicate that there is no pure rotation in natural mouth opening or closure, not even in the first millimeters of motion. The designation 'terminal hinge axis' should therefore be avoided and be replaced with 'kinematic axis'[14], as reported by Ferrario et al after kinesiographic observations[4]. The design basis for conventional articulators, which are based on the assumption of a terminal hinge axis, must be further questioned, and it is suggested that the ongoing development of virtual articulators should be based on biomechanical data such as ICR pathways. However, Gallo et al noticed a mismatch between the moving of the curve of the ICRs during mouth opening and closure, and explained it as different muscle activation[13,36]. In the present study, the deviation of both curves was confirmed. On closer examination of the first and last 10 degrees of mouth opening or closure, where occlusal guidance interferes with pure muscle activity, real-time MRI detected different ICR pathways, with higher spatial variability during mouth opening. In the present study of subjects without TMD symptoms, the trajectories of the ICRs (length, trail, curvature, inclination, and development of velocity) coincided to a high degree. These data could ideally be used to describe the physiologic biomechanical function of the TMJ, and in future studies to distinguish healthy subjects from patients with TMD by their ICR movement patterns. So far, kinetic analyses of the TMJ are informed by two-dimensional imaging of a three-dimensional movement; this is a limitation of the present real-time MRI study. The use of more than one MRI section at the same time might close this gap in the near future, enabling an even better characterization of TMJ structures during natural movement[22]. Moreover, the simultaneous visualization of both TMJs and the measurement of reproducibility during multiple movements might offer new and profound insights into the common functionalities of this multifarious joint in future studies.

Conclusion

Novel, real-time MRI of TMJ dynamics allows for a determination of ICR pathways as a useful method for characterizing joint biomechanics under physiologic conditions. Biomechanical data of ICR pathways might be useful for the development of virtual articulators. Analyses of ICR pathways might be beneficial for the detection of functional impairment in the future.

Disclaimer

JF holds a patent on the real-time MRI technique used in this article. All the other authors declare that there are no conflicts of interests.

References

1. Ahn SJ, Tsou L, Antonio Sánchez C, Fels S, Kwon HB. Analyzing center of rotation during opening and closing movements of the mandible using computer simulations. J Biomech 2015;48:666–671.
2. Ishigaki S, Nakamura T, Akanishi M, Maruyama T. Clinical classification of maximal opening and closing movements. Int J Prosthodont 1989;2:148–154.
3. Posselt U. Terminal hinge movement of the mandible. J Prosthet Dent 1957;7:787.
4. Ferrario VF, Sforza C, Miani A, Serrao G, Tartaglia G. Open-close movements in the human temporomandibular joint: does a pure rotation around the intercondylar hinge axis exist? J Oral Rehabil 1996;23: 401–408.
5. Nägerl H, Kubein-Meesenburg D, Fanghänel J, Thieme KM, Klamt B, Schwestka-Polly R. Elements of a general theory of joints. 6. General kinematical structure of mandibular movements. Anat Anz 1991;173:249–264.
6. Wu JB, Xu XM, Sheng JG. Analysis of the open-closing movement of the human temporomandibular joint. Acta Anat (Basel) 1988;133:213–216.
7. Gray H. Anatomy Descriptive and Surgical. London: Lea Brothers & Company, 1897.
8. Brotmann DN. Hinge axis, Part I. The transverse hinge-axis. J Prosthet Dent 1960:436–440.
9. Nyffenegger JW, Schärer P, Jahn E. Opening movements of the mandible. SSO Schweiz Monatsschr Zahnheilkd 1971;81:961–990.
10. Shanahan TEJ, Leff A. Mandibular and articulator movements. J Prosthet Dent 1966;16:62–72.
11. Beek M, Koolstra JH, van Ruijven LJ, van Eijden TM. Three-dimensional finite element analysis of the human temporomandibular joint disc. J Biomech 2000;33:307–316.
12. Bell KA, Miller KD, Jones JP. Cine magnetic resonance imaging of the temporomandibular joint. Cranio 1992;10:313–317.
13. Gallo LM, Airoldi GB, Airoldi RL, Palla S. Description of mandibular finite helical axis pathways in asymptomatic subjects. J Dent Relat Res 1997;76:704–713.
14. Kohno S. Analysis of condyle movements in the sagittal plane [in German]. Dtsch Zahnarztl Z 1972;27:739–743.
15. Sadat-Khonsari R, Fenske C, Kahl-Nieke B, Kirsch I, Jüde HD. Mandibular instantaneous centers of rotation in patients with and without temporomandibular dysfunction. J Orofac Orthop 2003;64: 256–264.
16. Shoup TE. Optical measurement of the center of rotation for human joints. J Biomech 1976;9:241–242.
17. Tymofiyeva O, Proff P, Richter EJ, et al. Correlation of MRT imaging with real-time axiography of TMJ clicks. Ann Anat 2007;189:356–361.
18. Lotzmann U, Kobes LW. On the influence of weight and point of gravity position of the mandibular recording bow on the course of axiographic tracings [in German]. Dtsch Zahnarztl Z 1988;43:S67–S70.
19. Tanaka E, van Eijden T. Biomechanical behavior of the temporomandibular joint disc. Crit Rev Oral Biol Med 2003;14:138–150.
20. Krohn S, Frahm J, Merboldt KD, Wassmann T, Joseph AA, Bürgers R. Diagnosis of disk displacement using real-time MRI: clinical report of two patients. J Prosthet Dent 2018;119:206–209.
21. Krohn S, Gersdorff N, Wassmann T, et al. Real-time MRI of the temporomandibular joint at 15 frames per second – A feasibility study. Eur J Radiol 2016;85:2225–2230.
22. Krohn S, Joseph AA, Voit D, et al. Multi-slice real-time MRI of temporomandibular joint dynamics. Dentomaxillofac Radiol 2018;48: 20180162.
23. Zhang S, Gersdorff N, Frahm J. Real-time magnetic resonance imaging of temporomandibular joint dynamics. Open Med Imaging J 2011;511:1–7.
24. Schafer RW. What is a Savitzky-Golay filter? [Lecture Notes]. IEEE Signal Processing Magazine 2011;28:111–117.
25. Madden HH. Comments on the Savitzky-Golay convolution method for least-squares fit smoothing and differentiation of digital data. Anal Chem 1978;50:1383–1386.
26. Abramowitz M, Stegun IA. Handbook of Mathematical Functions: With Formulas, Graphs, and Mathematical Tables. Applied mathematics series. Dover Publications, 1965:875–924.
27. Blaschke W, Müller HR. Ebene Kinematik. München: Oldenbourg, 1956.
28. Abramowitz M, Stegun IA. Handbook of Mathematical Functions: With Formulas, Graphs, and Mathematical Tables. Applied mathematics series. Dover Publications, 1965:9–64.
29. Orsini MG, Kuboki T, Terada S, Matsuka Y, Yatani H, Yamashita A. Clinical predictability of temporomandibular joint disc displacement. J Dent Res 1999;78:650–660.
30. Zhang S, Block KT, Frahm J. Magnetic resonance imaging in real time: advances using radial FLASH. J Magn Reson Imaging 2010;31:101–109.
31. Sadat-Khonsari R, Fenske C, Kahl-Nieke B, Kirsch I, Jüde HD. The helical axis of the mandible during the opening and closing movement of the mouth. J Orofac Orthop 2003;64:178–185.
32. Bernard N, Utz KH, Schmitt L. The intraoral determination of the sagittal condyle path inclination during face-bow recording [in German]. Schweiz Monatsschr Zahnmed 1995;105:18–23.
33. McMillan AS, McMillan DR, Darvell BW. Centers of rotation during jaw movements. Acta Odontol Scand 1989;47:323–328.
34. Seiler F, Hupfauf L. Reproducibility of terminal hinge axis points [in German]. Dtsch Zahnarztl Z 1973;28:775–780.
35. Gallo LM. Modeling of temporomandibular joint function using MRI and jaw-tracking technologies – mechanics. Cells Tissues Organs 2005;180:54–68.
36. Gallo LM, Brasi M, Ernst B, Palla S. Relevance of mandibular helical axis analysis in functional and dysfunctional TMJs. J Biomech 2006;39:1716–1725.
37. Bosman AE. Hinge Axis Determination of the Mandible: An investigation of the accuracy of mandibular hinge axis determination by the kinematic method as compared with substitutive approximations. Leiden: Stafleu & Tholen, 1974.

Die biomechanische Analyse von Kiefergelenkbewegungen mithilfe der Echtzeit-MRT-Technik

Schlüsselwörter: *Kiefergelenk, Unterkieferbewegungen, Biomechanik, Echtzeit-MRT, momentane Rotationszentren*

Zusammenfassung

Ziel: Im Rahmen der Biomechanik des Kiefergelenks wird die traditionelle Scharnierachsentheorie zunehmend durch die Theorie der momentanen Rotationszentren (ICR) ersetzt. Typischerweise basiert die Bestimmung der ICR auf theoretischen Berechnungen oder dreidimensionalen Approximationen von Finite-Elemente-Modellen.
Material und Methoden: Die Anwendung der Echtzeit-Magnetresonanztomografie (MRT) ermöglicht die Darstellung von natürlichen, physiologischen Bewegungen des Kiefergelenks mit 15 Bildern pro Sekunde. In dieser Studie wurde das Echtzeit-MRT-Verfahren verwendet, um die Biomechanik des Kiefergelenks während habitueller Unterkieferbewegungen bei funktionell unauffälligen Probanden zu analysieren, wobei der Fokus der Analyse auf den Kondylenbahnneigungswinkeln (HCI) und den ICR-Polbahnen lag. Der Wilcoxon-Rangsummentest wurde zur vergleichenden Analyse von ICR-Polbahnen der Kieferöffnungs- und der Kieferschlussbewegungen verwendet.
Ergebnisse: Der HCI-Mittelwert betrug 34,8° (± 11,3°), der Unterkiefer rotierte im Mittel 26,6° (± 7,2°). Bei Mundöffnungs- und Kieferschlussbewegungen von 10°–30° unterschieden sich die resultierenden x- und y-Translationen signifikant (10°–20°, x: $p = 0{,}02$ und y: $p < 0{,}01$; 20°–30°, x: $p < 0{,}001$ und y: $p = 0{,}01$). Bei einer Rotation von 0°–10° und bei Rotationen von mehr als 30° zeigten sich keine signifikanten Unterschiede in der x- und y-Translation. Die okklusionsnahen Bewegungen unterschieden sich nur im Hinblick auf die y-Translation ($p < 0{,}01$).
Schlussfolgerung: Die Echtzeit-MRT-Technik ermöglicht die Erfassung der Kiefergelenkstrukturen während physiologischer Unterkieferbewegungen ohne zusätzliche Hilfsmittel. Die Ergebnisse der vorliegenden Studie unterstützen die Theorie der ICR. Die statistische Analyse bestätigte, dass Mundöffnungs- und Kieferschlussbewegungen unterschiedlichen ICR-Polbahnen folgen, was durch Variation in der Muskelaktivität während gegenläufiger Bewegungsrichtungen zu erklären sein könnte. Die ICR-Bahnen waren innerhalb der maximalen interinzisalen Distanz (MID) und in Okklusionsnähe (NO) ähnlich, was auf eine begrenzte Dehnbarkeit der Gewebefasern (MID) und Determination durch Zahnkontakt (NO) zurückzuführen sein könnte.

Sebastian Krohn

Sebastian Krohn, Dr med dent
Department of Prosthodontics, University Medical Center, Göttingen, Germany

Jens Frahm, Prof Dr rer nat
Biomedical NMR, Max-Planck-Institute for Biophysical Chemistry, Göttingen, Germany

Alannah Mahler, DMD
Department of Prosthodontics, University Medical Center, Göttingen, Germany

Henning Dathe, Dr rer nat
Department of Medical Informatics, University Medical Center, Göttingen, Germany

Sam Sedaghat, Dr med
Institute of Diagnostic and Interventional Radiology and Nuclear Medicine, BG University Hospital Bochum, Germany

Dietmar Kubein-Meesenburg, Prof Dr med dent
Department of Prosthodontics, University Medical Center, Göttingen, Germany

Florian Linss, DMD
Department of Prosthodontics, University Medical Center, Göttingen, Germany

Torsten Wassmann, Dr med dent
Department of Prosthodontics, University Medical Center, Göttingen, Germany

Ralf Bürgers, Prof Dr med dent
Department of Prosthodontics, University Medical Center, Göttingen, Germany

Address Dr Sebastian Krohn, Department of Prosthodontics, University Medical Center Göttingen, Robert-Koch-Straße 40, 37075 Göttingen, Germany; Email: sebastian.krohn@med.uni-Göttingen.de